DTU Library

Calibration of the TUD Ku-band Synthetic Aperture Radiometer

Laursen, Brian; Skou, Niels

Link back to DTU Orbit

Calibration of the TUD K_u-band Synthetic Aperture Radiometer

Brian Laursen & Niels Skou

Danish Center for Remote Sensing, Electromagnetics Institute
Technical University of Denmark (TUD), B-348, DK-2800 Lyngby, Denmark..
Phone: (45) 45 88 14 44, Fax: (45) 45 93 16 34, E-mail: ns@emi.dtu.dk

ABSTRACT

The TUD Synthetic Aperture Radiometer is a 2-channel demonstration model that can simulate a thinned aperture radiometer having an unfilled aperture consisting of several small antenna elements. Aperture synthesis obtained by interferometric measurements using the antenna elements in pairs, followed by an image reconstruction based on an inverse Fourier transform, results in an imaging instrument without the need of mechanical scan. The thinned aperture and the non-scanning feature make the technique attractive for low frequency spaceborne radiometer systems, e.g. at L-band.

Initial measurements are presented, and images suitable for demonstration of calibration, like distributed targets, has been measured.

INTRODUCTION

The imaging principle has been demonstrated previously with success (Laursen & Skou, 1994) but not fully calibrated. The TUD demonstration model consists of a new calibrated 2-channel K_u-band correlation radiometer with two horn antennas and an antenna mounting structure enabling the horns to be mounted in relevant positions within a certain aperture. The interference pattern measurements are obtained by cross-correlating the signals from the two antennas, which produce a sample of the visibility function (the visibility function is the Fourier transform of the brightness temperature variation in the image). A total aperture synthesis is obtained by sequentially placing the two antenna elements in all required pairs of positions and measure the corresponding samples of the visibility function.

The one by one measurement of the visibility samples in the demonstration model thus requires the test scene and the electronics to remain stable for a considerable time - typically a few hours. Temperature regulation suitable for long term stability of the radiometers, and calibration signal paths are included in the electronics. An IF switch arrangement in front of the analogue correlators gives an opportunity to use the cross-correlator as a self-correlator (identical to a detector), and hereby calibrate the two radiometers as well as the correlators in a traditional way. Offsets on the output of the correlators are reduced by phase switching the local oscillator signals and properly de-modulate after the correlator.

To enable a practical distance between the aperture and the target the system has been used in a focused mode by having the antenna elements mounted on a curved rail. By rotating this rail around a vertical axis the full aperture can be covered.

The samplings distance is chosen so that all visiblity samples are measured. The maximum aperture is $36\,\lambda$ resulting in a synthetic beamwidth of $1.9°$ at nadir and an image size of 18 x 18 pixels.

THE TUD DEMONSTRATION MODEL

The TUD K_u-band 2 channel correlation radiometer employs two single sideband super heterodyne receivers, see Figure 1. The RF centre frequency is 16.25 GHz and the IF centre frequency is 250 MHz with a 100 MHz system bandwidth. The noise figure is 2.9 dB

Small circular dual mode horns with a $1.5\,\lambda$ diameter are used as antenna elements. The reconstructed image is $\pm19°$ from nadir. The dual mode horns are optimised to obtain identical radiation patterns in E- and H-plan within the reconstructed field of view, to allow the rotation of the antenna elements. Using a $1.58\,\lambda$ samplings distance between the antenna elements all visibility samples (including the lowest visibility samples) are measured, and problems with extrapolation of the lowest samples are avoided.

Temperature stabilised low noise preamplifiers are placed right after the horn antennas, followed by phase stable flexible microwave cables, to allow the placement of the antenna elements in all required positions.

In correlation techniques all local oscillator signals must be phase locked to measure the I & Q correlation between input signals (the I & Q correlation is the real and imaginary part of the complex cross correlation at zero time difference between the input signals). In a two channel correlation
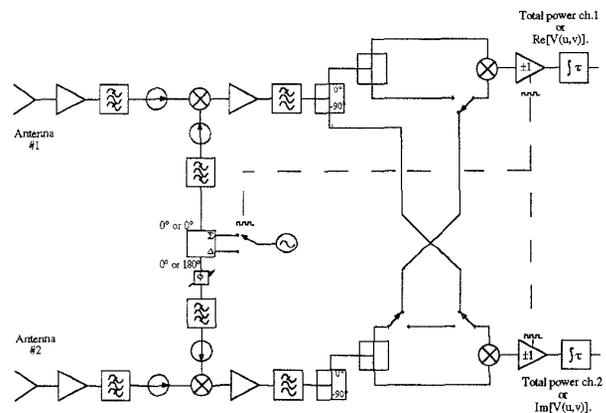

Figure 1. Block diagram of TUD K_u-band correlation radiometer.

812

radiometer this is achieved simply by using a common LO.

High isolation between the two channels is required and especially the LO section is critical. Isolation at RF as well as IF frequencies is obtained by a combination of isolators and waveguide filters. The LO filters are having two purposes, the IF isolation and a reduction of the phase noise (thermal noise) from the common LO by filtering at offset frequencies corresponding to the IF system band pass filter.

The power divider network used to feed the analogue correlators is also shown in Figure 1. In each channel it consists of a quadrature hybrid followed by in-phase 2-way power dividers. The analogue correlator is made by a four quadrant analogue multiplier and an integrator. An IF coax switch arrangement in front of the analogue correlators gives an opportunity to use the cross-correlator as self-correlator (identical to a detector), and hereby use the correlation radiometer as two total power radiometers (the position of the IF switches in Figure 1 corresponds to the situation where the radiometer is used as a two channel correlation radiometer). The calibration of the correlation radiometer is then performed in a traditional way when the radiometer is in total power mode.

Offset values on the output of the correlator is reduced by phase switching of the LO signals and proper demodulation after the correlator. The analogue integration time τ is 0.1 sec and the phase switching is done with $f_S = 1$ kHz.

Figure 1 shows the system with its analogue correlators, but the correlation radiometer is prepared for digital correlators as well. An extra 200 MHz LO section is included, and a 5-27 MHz output is available for digital correlators.

CALIBRATION

Talking about calibration of a correlation radiometer we will have to distinguish between systems using either analogue or digital correlators.

The output of the analogue correlator is proportional to the correlation between signals received by the antenna elements. Gain stability and gain calibration is crucial, while noise figure stability is less important as the noise from the receivers decorrelate.

The output of the digital correlator is a function of the correlation between the noise signals present at the input of the digital correlator. In that case a good stability of the noise figure is crucial. The rough quantisation for one, two or three bit correlators result in a significant non linearity between measured correlation and actual correlation (Thompson et al, 1986). This non linearity is theoretically well described and no critical problem. The number of quantisation levels for a digital correlator is for a spaceborne system a compromise between power consumption and sensitivity, ΔT. A one bit correlator has been chosen in the MIRAS design, an on-going ESA study. In that case gain stability is less important, as the one bit correlator only use the sign of the two noise signals being correlated.

An error correction is required, apart from the gain & noise figure calibration described above, to calibrate for hardware errors. The output from the correlator $V_e(\vec{u})$ can in both cases be given as eq.1, where $\vec{u} = (u_1, u_2)$ is the spatial frequency coordinates and (i,j) are the respective receivers

$$V_e(\vec{u}) = \left(Re[V] + j(Im[V]\cos(\beta) - Re[V]\sin(\beta))\right) e^{j\Delta\alpha} + V_{un\,i,j}$$

(1)

where V = $V(\vec{u})$ is the true visibility samples,
       $\Delta\alpha$ = $\alpha_i - \alpha_j$ phase errors before the 90° hybrid,
       β phase errors after the quadrature ,
       $V_{un\,i,j}$ DC offset on spatial frequencies.

The phase errors α_i and α_j can be corrected by software phase restoration as described in (Anterrieu et al, 1994). Phase errors on the 90° quadrature β must be solved in other ways. A simple solution for the digital correlator could be to place an extra correlator for every receiver (the number of extra correlators N is small compared to the total number of correlators N(N-1), where N is the number of receivers). As $V(\vec{u}) = V^*(-\vec{u})$, the correlation between i(0°) and j(-90°), and between i(-90°) and j(0°) is useful information to calibrate for phase errors after quadrature. Another solution could be to correlate i(0°) and i(-90°) and check if the result is zero, but it would be more critical to obtain isolation between i(0°) and i(-90°), than between i(0°) and j(-90°) and therefore less attractive.

The calibration of the gain and noise figure in the TUD K_u-band correlation radiometer is done with the IF switches in total power radiometer mode, and two external reference temperatures are used. The sky is used as a cold reference temperature by pointing the antenna element at zenith. As a warm reference temperature the antenna element is pointed at absorbers. At frequencies above X-band, the zenith sky temperature is no longer insensitive to the water vapour content in the atmosphere, and sky temperatures in the range of 6 to 15 Kelvin can be expected for a K_u-band radiometer. A third temperature can be applied with absorbers cooled by liquid nitrogen.

The spatial DC offset $V_{un}(i,j)$ is corrected by switching in uncorrelated noise in both receivers. The contribution to V_{un} is for the analogue correlator mainly coming from the offset current in the analogue multiplier. For the digital correlator, the contribution is mainly coming from offset voltages on the input of the 1 bit AD converter.

IMAGE RECONSTRUCTION

As measurements in the synthetic aperture radiometer are performed in the spatial frequency domain, a Fourier transform is used to come back to the spatial domain (the image domain). The spatial frequencies are in most cases not placed on a rectangular grid, except the T-shaped antenna, and a traditional inverse fast Fourier transform is therefore not suitable.

An inverse transform is in the general case given by (Anterrieu et al, 1994) where T_B is the brightness temperature

$$\frac{T_B(\vec{\xi})}{4\pi} \frac{G(\vec{\xi})}{\sqrt{1 - \|\vec{\xi}\|^2}} = \sum_{\vec{u} \in L_*} \hat{B}\left(\frac{u_1}{\Delta u}\right)\hat{B}\left(\frac{u_2}{\Delta u}\right)\frac{V(\vec{u})}{\rho(\vec{u})}e^{i2\pi\vec{u}\cdot\vec{\xi}}$$

(2)

813

where $\hat{B}(\upsilon)$ $= F\{B(\zeta)\}$, an interpolation function,

$G(\xi)$ the normalised antenna element pattern,

ξ $= (\xi_1,\xi_2) = (\sin\theta\cos\phi, \sin\theta\sin\phi)$.

L_e is the list of measured spatial frequencies, and $\rho(\bar{u})$ is taking care of local redundancy or in a more general case like Figure 2 a cluster of visibility samples especially at the centre

$$\rho(\bar{u}) = \sum_{\bar{u}' \in L_e} \hat{B}^2\left(\frac{u_1-u_1'}{\delta u}\right)\hat{B}^2\left(\frac{u_2-u_2'}{\delta u}\right) \tag{3}$$

A fast Fourier transforms is required for large synthetic apertures to reduce the computation time, and several are available apart from the rectangular FFT. The hexagonal FFT is useful in the case of a Y-shaped antenna, and a Hankel FFT can be used on the geometry in Figure 2.

DISCUSSION OF THE IMAGE

In Figure 3 is shown the first result from the K_u-band correlation radiometer, imaging a specially designed two level brightness temperature scene. High temperatures of 280 Kelvin emanate from absorbers and a metal plate reflecting the sky temperature is the low temperature of 20 Kelvin. The metal plate placed at the centre is 22.5 vs. 28 cm (5 vs. 6 pixels). Point targets are useful for testing resolution while the distributed target as discussed here serves as test object for the calibration accuracy assessment.

Ripples are seen in the image, in the absorber area at the edge as well as in the cold area. The demonstrated calibration accuracy at the edge is in the range of 15 K. Offset errors in
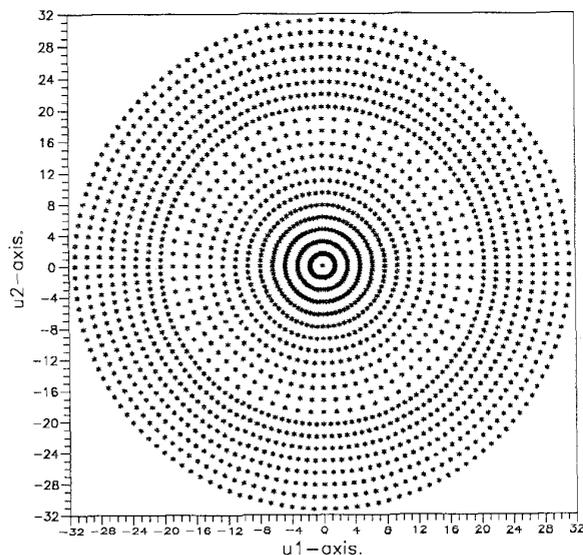
the frequency domain are the main reason for the errors in the centre.

CONCLUSIONS

2 dimensional reconstruction of interferometric radiometer imagery has been carried out with success, however with little emphasis on calibration fidelity. The present work is focussed on these issues. A first target has been measured and priliminarily evaluated. Further work on algorithms and measurements of other specialised targets is in progress.

ACKNOWLEDGEMENT

REFERENCES

Anterrieu, E., Lannes, A.: "Instrument Modelization, Antenna Geometry and Algorithms." MIRAS working document, March 1994.

Laursen, B., Skou, N.: "A Spaceborne Synthetic Aperture Radiometer Simulated by the TUD Demonstration Model", IGARSS'94, pp 1314-1316.

Thompson, A.R., Moran, J.M., Swenson, G.W.: "Interferometry and Synthesis in Radio Astronomy." JOHN WILEY & SONS, 1986.

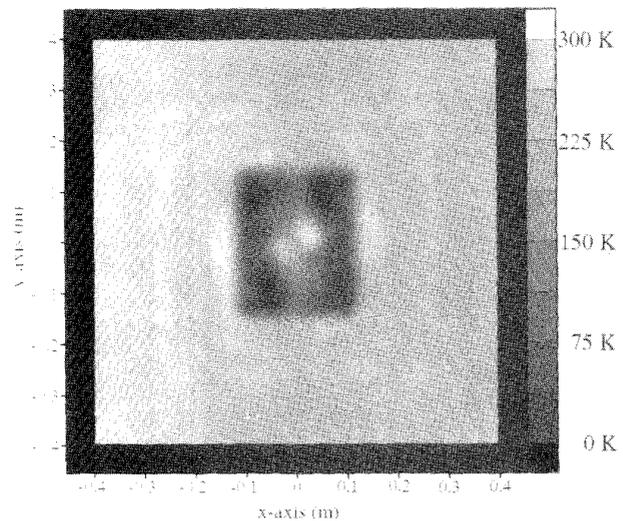Figure 2. Measured spatial (u_1,u_2) frequencies for the near-field set-up.

Figure 3. 5 vs. 6 pixels metal plate reflecting the sky temperature is imaged by the near-field set-up.